Site specific deacylation by ABHD17a controls BK channel splice variant activity

Site specific deacylation by ABHD17a controls BK channel splice variant activity

Heather McClafferty, Hamish Runciman & Michael J Shipston

Centre for Discovery Brain Sciences, Edinburgh Medical School: Biomedical Sciences, University of Edinburgh, Edinburgh EH8 9XD

Running title: Site specific deacylation of BK channels by ABHD17a

Corresponding author:
Michael J Shipston
Centre for Discovery Brain Sciences
Edinburgh Medical School: Biomedical Sciences
University of Edinburgh
Edinburgh, UK
EH8 9XD
email: mike.shipston@ed.ac.uk
Tel: +44 131 6503253

Keywords: *S*-acylation, palmitoylation, acyl thioesterase, potassium channel, ion channel, Kcnma1, Kcnmb1, post-translational modification, lipid modification, protein trafficking

Abstract

S-acylation, the reversible post-translational lipid modification of proteins is an important mechanism to control the properties and function of ion channels and other polytopic transmembrane proteins. However, while increasing evidence reveals the role of diverse acyl protein transferases (zDHHC) in controlling ion channel S-acylation the acyl protein thioesterases that control ion channel deacylation are very poorly defined. Here we show that the α/β-hydrolase domain-containing protein 17a (ABHD17a) deacylates the STREX domain of large conductance voltage- and calcium-activated potassium (BK) channels inhibiting channel activity independently of effects on channel surface expression. Importantly, ABHD17a deacylates BK channels in a site-specific manner as it has no effect on the S-acylated S0-S1 domain conserved in all BK channels that controls membrane trafficking and is deacylated by the acyl protein thioesterase Lypla1. Thus, distinct S-acylated domains in the same polytopic transmembrane protein can be regulated by different acyl protein thioesterases revealing mechanisms for generating both specificity and diversity for these important enzymes to control the properties and functions of ion channels.

Introduction

Protein S-acylation, the dynamic and reversible postranslational modification of cysteines residues through addition of a fatty acid (typically the 16-carbon fatty acid palmitate) via a labile thioester bond, is an important modulator of the lifecycle of many polytopic transmembrane proteins including receptors, transporters and ion channels (1–4). Indeed, a large repertoire of pore-forming and accessory ion channel subunits are known to be S-acylated controlling diverse channel properties and functions from assembly, through trafficking to the cell surface, to regulation by diverse signalling cascades. S-acylation is mediated by a family of transmembrane zinc DHHC (Asp-His-His-Cys) acyl transferases (zDHHC) (5–7). For many transmembrane proteins we are beginning to understand the repertoire of zDHHCs that can show some selectivity for different ion channels and even S-acylated domains in the same protein. In contrast, there is a dearth of evidence for the acyl protein thioesterase enzymes that remove lipids from (deacylation) most polytopic transmembrane proteins including ion channels. Classically, two members of the serine hydrolase superfamily (LYPLA1 and LYPLA2) were thought to be the major acyl protein thioesterases that mediate deacylation of cytosolic cysteine residues in proteins even though it was clear many proteins were not controlled by these enzymes (8–10). Indeed, additional members of the broader serine hydrolase family, in particular the α/β-hydrolase domain-containing protein 17 (ABHD17) family, have been identified by activity profiling and shown to be functional acyl protein thioesterases that are targeted to the plasma membrane and deacylate a number of peripheral membrane and other proteins including Psd-95, N-Ras, Gap-43, and Map6 (11–14). However, the regulation of polytopic transmembrane proteins, including ion channels, by α/β-hydrolase domain-containing protein or other acyl protein thioesterases of the serine hydrolase family, and whether they display specificity, is essentially unknown.

We have previously revealed that the trafficking, function and regulation of pore forming subunit (Kcnma1) of the large conductance calcium- and voltage activated potassium (BK) channel is controlled by S-acylation of two distinct domains (Figure 1A). The intracellular loop between transmembrane domains S0 and S1 (S0-S1 loop) is S-acylated at a cluster of conserved cysteine residues that controls trafficking to the plasma membrane and functional assembly with regulatory β1-accessory subunits (15, 16). This domain is largely S-acylated by zDHHC23 that promotes membrane trafficking of the α-subunit alone and is a target for deacylation by Lypla1 resulting in channel retention in the trans Golgi network (15). In contrast, the alternatively spliced stress regulated exon (STREX) introduces an additional conserved tandem cysteine motif that is S-acylated by a number of zDHHCs, including zDHHC17, but not zDHHC23 (17–19). S-acylation of the STREX domain enhances the apparent calcium sensitivity of the channel (17–19) and determines STREX variant channel regulation by AGC-family protein kinase dependent phosphorylation (17, 20). However, acyl protein thioesterases that deacylate the STREX domain have not been identified.

In this manuscript we sought to i) characterise acyl protein thioesterases that deacylate the STREX domain; ii) to establish whether these acyl transferases display specificity between the STREX and S0-S1 loop domains and iii) determine the functional impact of identified acyl protein thioesterases on channel trafficking and function. We demonstrate that ABHD17a is an acyl protein thioesterase that deacylates the STREX, but not S0-S1, domain of BK channels and in accordance with its specificity for the STREX domain controls channel activity rather than channel trafficking.

Results

ABHD17a deacylates the BK channel STREX domain

To define potential acyl thioesterases that control deacylation of the STREX domain of BK channels we first employed an imaging based screen that we have previously exploited to identify acyltransferases that S-acylate the STREX domain (17). In these assays we expressed the intracellular STREX-CRD domain of the BK channel (Figure 1B) as a -GFP fusion protein in HEK 293 cells. As previously reported, expression of the isolated STREX-CRD domain results in robust expression of the fusion protein at the plasma membrane of HEK293 cells (Figure 1C) due to endogenous S-acylation of the fusion protein (17). Membrane expression of the fusion protein is completely abolished by site directed mutagenesis of the tandem S-acylated cysteine residues (Cys^{645} and Cys^{646}) to alanine in the STREX domain (STREX-CRD-C645:646A) resulting in predominantly cytosolic membrane expression.

To examine potential acyl thioesterases that deacylate the STREX domain we co-expressed the STREX-CRD fusion protein with a battery of candidate acyl thioesterases (Figure 1D and 1E) including members of the ABHD (11, 21) and classical LYPLA families that showed robust expression in our HEK293 cell assay system (Figure 1D). Although activity based profiling and functional assays have suggested that the ABHD17 family, as well as ABHD12 and ABHD13, may have thioesterase activity against S-acylated proteins for the vast majority of ABHD family proteins their S-acyl thioesterase or other functions are not known (8, 11, 12). For example, ABHD 12 has also been shown to be a lysophopsholipid lipase whereas the function of ABHD13 is not known. Significantly out of 19 putative acyl thioesterases tested only ABHD17a and ABHD17c had a significant effect on reducing membrane expression of the STREX-CRD fusion as predicted for an acyl thioesterase that deacylates the STREX domain. ABHD17a and 17c have both been reported to control deacylation of a number of peripheral plasma membrane associated proteins (11, 21). However, expression of ABHD17a resulted in a larger and more consistent reduction in membrane expression of the STREX-CRD fusion protein compared to ABHD17c (Membrane expression expressed as a fraction (Mean $\pm$ SD) of that for STREX-CRD alone was: for ABHD17a 0.38 ± 0.21 n = 28 and ABHD17c 0.57 ± 0.33, n = 24, $p<0.05$ Kruskal Wallis with post-hoc Dunns test). In contrast, although ABHD17b was robustly expressed in HEK293 cells (Figure 1D), this closely related ABHD family member had no significant effect on STREX-CRD membrane association. Moreover, Lypla1 and Lyplal1 that we have shown previously (15) can deacylate the S0-S1 loop of BK channels, had no significant effect on STREX-CRD membrane localisation.

To address whether ABHD17a and ABHD17c in fact deacylate the STREX domain of BK channels we used acyl-RAC assays to address acylation of the full length BK channel expressed in HEK293 cells in the presence and absence of ABHD17a and ABHD17c. In addition, we addressed whether ABHD17a or ABHD17c is specific for the STREX domain by assaying whether overexpression of these acyl thioesterases will also deacylate the S0-S1 loop domain of the BK channel to ask if these ABHDs show specificity for distinct sites in the same polytopic transmembrane protein.

We first assayed whether the S0-S1 domain is deacylated by ABHD17a and 17c by expressing the ZERO variant of the BK channel. The ZERO variant is identical to the STREX variant except that it lacks the alternatively spliced STREX insert but is S-acylated at the conserved S0-S1 loop. In control cells ZERO channels display robust and specific pull down in acyl-RAC assays only when the thioester bond between the endogenous lipid and the cysteine residues in the S0-S1 loop has been cleaved by hydroxylamine ($+NH_2OH$) (Figure 2A). However, neither overexpression of ABHD17a or ABHD17c had any significant effect on ZERO channel pull down by acyl-RAC assay (Figure 2C) demonstrating the S0-S1 loop is not a target for these ABHDs.

To address if the STREX domain is specifically deacylated by ABHD17a or ABHD17c we expressed STREX channels in which the S-acylation sites in the S0-S1 loop have been mutated to alanine (STREX-C53:54:56A construct). STREX-C53:54:56A channels are robustly S-acylated and thus pulled down in acyl RAC assays from control HEK293 cells (Figure 2B). Overexpression of ABHD17a and 17c both resulted in a significant (Figure 2B) reduction in S-acylated STREX-C53:54:56A channels captured in these assays (S-acylation expressed as a percentage of STREX-C53:54:56A alone was: for ABHD17a $26.8 \pm 14.1\%$, n= 4, $p< 0.01$ and for ABHD17c $57.5 \pm 25.9\%$, n= 4, $p< 0.05$ Kruskal Wallis with post hoc Dunn's test). This supports the data form our imaging screen that ABHD17a and 17c deacylate the STREX domain to control its association with the plasma membrane.

ABHD17a or 17c do not control surface expression of STREX BK channels

The acyl-RAC data suggest that ABHD17a and 17c act specifically on the STREX domain of the BK channel, and have no effect on the S-acylation of the S0-S1 loop of the BK channel. To further test this specificity we first addressed whether ABHD17a or 17c controlled the surface expression of the BK channel. BK channel surface expression is attenuated in channels that are deacylated at the S0-S1 loop, as a result of increased retention in the trans Golgi network (15). To assay BK channel surface expression we exploited an on-cell Western approach to assay surface expression of epitope tagged BK channels in cell population assays (16, 22). In these assays, the Flag- epitope at the extracellular N-terminus of the BK channel is used to assay channels that are resident at the cell surface in intact cells, whereas the -HA epitope at the intracellular C-terminus of the channel allows assay of total BK channel expression in the same cells following cell permeabilization. The ratio of Flag to HA signal thus provides a reporter of BK channel surface expression as a function of total channel expression.

We first assayed cell surface expression of the ZERO variant of the BK channel that lacks the STREX domain (Figure 3). In agreement with previous studies (15) co-expression with the cytosolic acyl thioesterase Lypla1 resulted in a significant reduction in ZERO channel surface expression as predicted as a result of deacylation of the S0-S1 loop (Figure 3B). In the presence of Lypla1 ZERO channel surface expression was 0.28 ± 0.07 fold, n = 5 of ZERO channels alone. Surprisingly, overexpression of ABHD17a, but not ABHD17c, caused a small but significant increase in ZERO channel surface expression (Figure 3A & 3B). However, this increase in surface expression was also observed with the catalytically inactive mutant of ABHD17a in which S170 and D255 in the catalytic triad were mutated to alanine (ABHD17a-mut) suggesting the enhancement of surface expression is not dependent on deacylation *per se* (Figure 3A & 3B). In further support of this deacylation independent effect, overexpression of ABHD17a-mut also had a small but significant enhancement of BK channel surface expression in ZERO channels that are S-acylation null (ZERO-C53:54:56A) ruling out deacylation of the channel itself is involved in this stimulatory effect on surface expression (Figure 3A & 3D). ZERO, or ZERO-C53:54:56A, channel surface expression was not enhanced by the truncation mutant of ABHD17a (Δ19-ABHD17a) in which the N-terminal 19 amino acids, that includes S-acylated cysteines important for membrane targeting (11), has been deleted (Figure 3A, 3B & 3D). Taken together, this unexpected enhancement of ZERO channel surface expression likely results from either a chaperone effect on the channel or a potential dominant negative effect of ABHD17a catalytic mutants on other components of the BK channel trafficking pathway.

In contrast, ABHD17a, its catalytic or membrane targeting mutants, nor ABHD17c had no effect on STREX or STREX-C53:54:56A channel membrane expression (Figure 3A, 3C & 3E). Taken together, these data demonstrate that ABHD17a or 17c do not inhibit BK channel surface expression through deacylation of the S0-S1 site in accordance with the lack of effect of these enzymes on S0-S1 loop S-acylation in acyl-RAC assays.

To test if the unexpected ABHD17a deacylation independent enhancement of ZERO channel surface expression was a result of reduced ZERO channel internalisation we exploited a population based assay of BK channel internalisation in HEK293 cells (16). ZERO BK channels at the cell surface were labelled at their extracellular N-terminal Flag- tag epitope and allowed to internalise for 60 mins at 37°C before stripping of cell surface label allowing quantification of ZERO channel internalisation (Figure 4A). Approximately 30% of surface expressed ZERO BK channels internalised over this 60 minute assay in control HEK293 cells (Figure 4B & C). Overexpression of ABHD17a, or its catalytic (ABHD17a-mut) or membrane targeting (Δ19-ABHD17a) mutant had no effect on ZERO channel internalisation (Figure 4C). This indicates that the enhancement of ZERO channel surface expression is likely due to deacylation independent effects of ABHD17a on forward trafficking and/or delivery of the channel to the plasma membrane rather than through decreased internalisation or stability at the plasma membrane.

Deacylation of STREX domain by ABHD17a controls channel activity at the plasma membrane

As ABHD17a had no effect on STREX channel surface expression we asked whether ABHD17a mediated deacylation of STREX has an effect on BK channel function and activity. We have previously shown that channels that cannot be S-acylated in the STREX domain are less sensitive to physiological voltages and intracellular free calcium levels compared to wild-type STREX channels (17, 19). To assay the effect of ABHD17a on STREX channel function we used a membrane potential assay in HEK293 cells in which heterologously expressed BK channels are stimulated upon calcium entry mediated through the calcium ionophore ionomycin (23, 24). In this assay simulation of mock transfected cells with ionomycin results in depolarisation of the

membrane potential (Figure 5A) over the 180s time course of the assay as a result of calcium influx. Overexpression of ABHD17a had no significant effect on the time course or magnitude of the ionomycin-induce depolarisation of mock transfected HEK293 cells (Figure 5A). In cells overexpressing STREX channels ionomycin results in a rapid and transient hyperpolarisation of the membrane potential that typically remains significantly hyperpolarised compared to mock transfected cells over the time course of the assay (Figure 5A). Co-expression of ABHD17a with STREX channels resulted in a significantly attenuated peak hyperpolarisation in response to ionomycin (Figure 5A & 5B) that is ~ 60% smaller than the peak hyperpolarisation observed with STREX channels expressed alone. In the presence of STREX and ABHD17a the peak HEK293 hyperpolarisation was 0.41 ± 0.12 fold, n = 20, ** p< 0.01 Kruskal Wallis with post hoc Dunn's test compared to HEK293 cells expressing STREX channels alone. Importantly, the inhibitory effect of ABHD17a on STREX channel activity was completely abolished using the catalytically inactive ABHD17a mutant (ABHD17a-mut) (Figure 5B). Moreover, the peak hyperpolarisation observed on co-expression of STREX channels with ABHD17a was similar to that observed in STREX channel S-acylation null mutants that cannot be S-acylated in the STREX domain (STREX-C645:646A). Furthermore, ABHD17a had no significant effect on the hyperpolarisation induced by ionomycin in STREX-C645:646A expressing HEK293 cells confirming the inhibitory effect is mediated via deacylation of the STREX domain. Taken together, these data reveal that ABHD17a specifically deacylates the STREX domain of BK channels resulting in functional inhibition of STREX channel activity.

Discussion

Using a combination of an imaging-based screen, acyl-RAC and functional assays of BK channel trafficking and activity we reveal that ABHD17a is a major acyl protein thioesterase that site specifically deacylates the STREX domain of the BK channel to control channel activity. Together with previous work (15), these data reveal that in the same polytopic transmembrane protein different acyl protein thioesterases can control distinct sites with diverse functional impacts on channel behaviour. In the case of BK channels ABHD17a controls STREX domain and channel activity whereas Lypla1 (and a splice variant of Lyplal1) controls the S0-S1 domain and channel trafficking/functional coupling to β-subunits (15, 16) (Figure 6A). Strikingly, these domains are also regulated by distinct acyl protein transferases supporting an increasing body of evidence that both acyltransferases and acyl protein thioesterases can display some target specificity as well as more promiscuous behaviour.

To date, the majority of ABHD17 family targets for deacylation include a number of peripheral membrane proteins, that are targeted to plasma membranes via S-acylated domains such as Psd-95, N-Ras and Mpp6 (11, 12, 14), rather than transmembrane proteins (Figure 6B). However, while ABHD17 members have been shown to display some selectivity between different proteins the mechanism(s) by which such selectivity may occur is not known. Moreover, how ABHD17a and Lypla1 respectively may discriminate between between the S0-S1 and STREX domains in BK channels remains unclear. Several potential mechanisms may be involved. Firstly, although some reports have suggested that Lypla1 can target the plasma membrane the majority of studies suggest it is a largely cytosolic protein whereas ABHD17a-c have a highly S-acylated N-terminus and shown to target in plasma membranes in a variety of cell types (9, 10). Thus, differential local accessibility of distinct BK channel loop domains from a cytosolic vs peripheral membrane location, or differential association of Lypla1 and ABHD17a with these distinct BK channel domains, may provide a mode of discrimination in cells.

Secondly, ABHD targets defined to date (Figure 6B) have candidate target cysteine residues in either the N- or C-terminal tails of peripheral membrane proteins there is no clear amino acid sequence consensus that might suggest discrimination of ABHD17 targets from other acyl thioesterases. Indeed, the classical acyl thioesterases Lypla1 and Lypla2 show both distinct and overlapping targets in accordance with their structural and sequence conservation with very similar surface polarity and substrate binding regions (25). Lypla2 is likely more flexible than Lypla1 and as both have a single acyl binding pocket may explain preference of both enzymes for mono-acylated substrates but both have reduced activity. However, recent studies using short fluorogenic peptides in assay screens has provided some insight into vicinal amino acids surrounding a single cysteine amino acid that may change the efficiency of hydrolysis between Lypla1 and Lypla2. For example, positively charged residues in the downstream P1' and P2' positions enhance hydrolysis whereas bulky aromatic residues in the upstream P1 and P2 positions limit hydrolysis (26). Previously identified ABHD family targets (Figure 6B) have residues vicinal to S-acylated cysteines that would not, in general, be highly favourable for

hydrolysis by Lypla1 or Lypla2. However, the extent to which similar rules might apply to ABHD17 remains to be determined. Intriguingly in our assays ABHD17b had no effect on the STREX domain in our imaging screens whereas it is the major enzyme controlling PSD-95 deacylation (12). Thus, how potential differences in deacylation efficiency between ABHD17 isoforms remains to be explored.

Furthermore, whether ABHD or Lypla family acyl protein thioesterases have differential effects when target cysteines are in clusters of di-cysteine motifs remains to be examined. Again, available sequences of ABHD17 target proteins (Figure 6B) reveal that proteins with both clusters or di-cysteine motifs are targets such, as in the STREX domain, or in targets with lone cysteine residues. Moreover, the efficiency with which acyl thioesterases can catalyse hydrolysis of bound lipid species (depending on carbon backbone length or saturation) may also play an important role as in most cases the endogenous lipid, although often assumed to be palmitate, is not known for most S-acylated sites in proteins.

The ability of different acyl protein thioesterases to target distinct S-acylated domains in the same polytopic transmembrane protein suggest that deacylation of these two domains may be both spatially and temporally controlled as has been proposed for peripheral membrane proteins such as N-Ras and Psd-95 as well as the microtubule binding protein MAP6 (12, 27). The extent to which deacylation of these domains in BK channels is “constitutive’, dependent on the relative activity of competing zDHHC and acyl thioesterases, or might itself be dynamically controlled for example by environmental and/or signalling induced modulation of acyl protein thioesterase location and/or activity remains to be explored (28).

In the course of these studies we observed a consistent and significant effect of catalytically inactive (ABHD17a-mut), but not inappropriately targeted Δ19-ABHD17a to enhance the surface expression of the ZERO variant of BK channels. This small stimulatory effect on surface levels was not observed in the BK channel STREX suggesting that overexpression of the catalytically null ABHD17a has distinct effects on the trafficking pathways controlling ZERO and STREX variant surface expression. Although S-acylation of the S0-S1 domain has been reported to modify lateral mobility and surface expression of BK channels (29, 30) ABHD17a-mut had no effect on ZERO channel internalisation. Furthermore, this small enhanced surface expression upon ABHD17a-mut overexpression was also observed in S-acylation deficient ZERO BK channels (C53:54;56A) demonstrating this is independent of ZERO channel S-acylation but may result from changes in forward trafficking. Whether, overexpression of ABHD17a-mut results in affects on other components of the BK channel trafficking pathway, may act as a potential chaperone or may result from other activities or binding partners of ABHD17a warrants further investigation. For example, both Lypla1 and Lypla2, along with other ABHD family members display diverse functions, including hydrolysis of other lipids (8) but likely are functional monomers (25). Irrespective of mechanism, it does suggest that differences in forward trafficking for ZERO and STREX channels may exist.

In summary, we have identified ABHD17a as a major acyl protein thioesterase that deacylates the STREX domain of BK channels to control channel activity independently of changes in cell surface expression. As ABHD17a and Lypla1 target different domains of the BK channel this may: i) provide a suitable model to understand the rules controlling efficiency of acyl protein thioesterase to hydrolyse thioester lipid linkages in membrane proteins and ii) allow us to unmask the mechanisms by which deacylation of distinct BK channels domains may control BK channel physiology and function.

Experimental procedures

Reagents

General biochemical reagents used throughout this study were obtained from Sigma-Aldrich and were of analytical-grade quality unless stated otherwise.

HEK 293 cell culture and transfection

HEK 293 cells were originally obtained from ATCC and cultured and transfected essentially as previously described (15–17). The cells were maintained in DMEM containing 10% fetal bovine serum (both Life Technologies), incubated at 37 °C in 5% CO_2 and used between passage 18 and 30. HEK293 cells used in this study do not express endogenous BK channel subunits as determined by mRNA, protein, or functional assays (15–17). For transfection, cells were typically plated on 6-well plates for 24 h before transfection with corresponding plasmid cDNA using PolyJet (tebu-bio). In all co-transfection assays channel cDNAs were transfected at a 1:1 ratio with acyl thioesterases or empty pcDNA3.1 plasmid in controls.

BK channel and acyl thioesterase constructs

The generation of BK channel ZERO and STREX variant subunits with an extracellular N-terminal FLAG- and intracellular C-terminal -HA epitope

tags in pcDNA3, together with S-acylation deficient site directed mutants and the STREX-CRD domain as a -YFP fusion have been described previously (15–17). Original ABHD family clones as Flag-tagged constructs in the pCAGGS vector were a generous gift of Professor Masaki Fukata (21) and used in the initial imaging screens in Figure1. Lypla1, Lypla2 and Lyplal1 clones were as previously described (15). A catalytically inactive version of ABHD17a was made by mutating amino acids S170 and D255 in the catalytic triad to alanine by synthesising the entire coding sequence (Twist Bioscience) containing the mutated amino acid codons and incorporating the FLAG tag and restriction sites EcoRI and NotI flanking the coding sequence and subcloned into pcDNA3.1. The targeting deficient ABHD17a mutant (11, 21) that lacks the first 19 amino acids at the N-terminus including S-acylated cysteine residues required for membrane targeting (∆19-ABHD17a) was generated by PCR using a forward primer containing an EcoRI restriction site and a start methionine, 5'-AAAGAATTCACCATGGGCCGCATCGCGCGGCCAAG-3', and a reverse primer to amplify a KpnI site in the original sequence 5'-CCACTGCAGCACACTCATAACG-3' were used to PCR amplify the clone, subcloning back into an empty pCAGGS vector. For assays in which ABHD17a enzymes were co-expressed with Flag- and -HA epitope tagged BK channels the Flag tags of the corresponding full length ABHD17a clones was engineered to a myc-epitope tag by PCR. Briefly, full length constructs were amplified by PCR using the primers, Forward (including a BamHI site) 5'-GCCGGATCCGGCCACCATGAACGGCCTGTCGGTGAGCGAGCTC-3' and Reverse (including a XbaI site) 5'-TGGTCTAGATTA*CAGATCCTCTTCTGAGATGAGTTTTTGTTC*GGTGCGTTGG-3' and the amplicons subcloned into pcDNA3.1. To generate myc tagged ∆19-ABHD17a, the forward primer used to generate ∆19-ABHD17a was used with the myc reverse primer and cloned into pcDNA3.1 by restriction digest using EcoRI and XbaI. All clones were validated by DNA sequencing.

STREX-CRD imaging assay

Cells were processed, imaged and quantified essentially as described (17). In brief, HEK293 cells were plated on glass coverslips, transfected as above and 48h later fixed with 4% ice-cold paraformaldehyde for 15 min at room temperature. After quenching with 50 mM NH_4Cl, cells were either first probed for the epitope tag of the corresponding acyl thioesterase before mounting on microscope slides using Mowiol or Fluorsave. Cells were initially screened using an epifluorescence microscope with a 100x oil objective lens. Confocal images were acquired on either a Nikon A1 or Zeiss LSM510 laser scanning microscope, using a 63x oil Plan Apochromat (N.A. = 1.4) objective lens. The majority (> 90%) of experiments were performed blind by an observer independent from the experimentalist undertaking the cell transfections. Membrane expression was typically observed in >95% of HEK293 cells transfected with the STREX-CRD fusion protein. To determine membrane expression upon co-expression with putative acyl thioesterases line scans of fluorescent intensity through 4 independent areas of the plasma membrane, cytosol and nucleus of cells were analyzed using Fiji software (NIH). To determine plasma membrane localisation a signal intensity at the cell periphery that was 2 SD greater than that in the cytosol in any of the 4 planes was defined as a cell with membrane expression. For each coverslip 3–5 random fields of view were analyzed to determine the number of transfected cells with plasma membrane localization of the STREX-CRD fluorescent fusion protein. The average percentage of transfected cells from each coverslip (minimum 50 cells per coverslip) that displayed membrane expression was then normalized to the corresponding wild-type STREX-CRD control in each independent experiment.

On cell Western cell surface expression assays

Assays were carried out as described previously (16, 22). Transfected HEK293 cells were plated into a 96 well poly-d-lysine coated, black walled, clear bottom plate (Greiner) and assayed 48 h post-transfection. Cells were stained on ice in growth medium (GM: DMEM + 10% foetal bovine serum) for the FLAG epitope applying mouse anti-FLAG-M2 (Sigma, 1:100 in GM), then washed in GM and stained for 1 h with anti-mouse IRDye800CW goat IgG (Licor, 1:100 in GM). Cells were then fixed, permeabilized and blocked in Odyssey Blocking Buffer (OBB) before staining at room temperature for 1 hr with anti-HA antibody (Immune Systems, 1:1000 in OBB) followed by anti-rabbit secondary IRDye690RD (Licor, 1:500 in OBB). Separate wells were stained with TO-PRO™-3-iodide (1:500) to account for cell number. Cell staining was imaged on an Odyssey IR imager and were analyzed using Image Studio Lite Ver5.2 (freeware from Licor). Staining intensity was normalized to cell number and background-subtracted before calculating the ratio of surface FLAG:HA total protein staining.

BK channel internalization assay

Assays were carried out as described previously (16). Transfected HEK293 cells were plated into

a 96 well poly-d-lysine coated, black walled, clear bottom plate (Greiner) and assayed 48 h post-transfection. All cells were stained on ice for the FLAG epitope, anti-FLAG-M2 (1:100 in DMEM + 10% foetal bovine serum (GM)), washed in GM then stained with anti-mouse IRDye800CW (1:1000 in GM). Ice-cold stripping buffer (0.1 M glycine, 0.1 M NaCl, pH 2.5, in PBS) was immediately applied to a subset of wells and then washed in growth medium to determine background staining. To allow endocytosis and internalization of labelled channels to occur, cells were incubated at 37 °C in a humid chamber for 1 h. The cells were then cooled on ice and a subset of cells were stripped to measure internalized staining with a further subset remaining unstripped to measure total FLAG staining. All cells were then stained for 30 mins on ice with NucRed™ Live 647 ReadyProbes™ reagent (ThermoFisher) to account for cell number. Cells were imaged on an Odyssey IR Imager and analyzed using Image Studio Lite version 5.2. For each well, staining intensity of FLAG was normalized to the NucRed signal. Background signal detected in time 0 stripped cells (*i.e.* no internalization) was averaged and subtracted from the other wells. Remaining signal detected after stripping treatment in the 60 min, 37 °C incubation wells was then normalized to the total surface staining in the unstripped wells, and expressed as a percentage of total BK channel surface expression without stripping.

Acyl-RAC of BK channel S-acylation

Acyl-RAC experiments were based on the protocol as previously described (15, 31). Transfected cells were lysed 48 h post transfection in blocking buffer (100 mM HEPES, 1 mM EDTA, and 2.5% SDS, pH 7.5), disrupting cells using a 21-gauge needle and syringe for 20 strokes. Lysates were treated with 0.1% methanethiosulfonate (MMTS) and incubated for 4 h at 40 °C with shaking. Proteins were precipitated in acetone and stored at -20 °C overnight before washing five times in 70% acetone to remove the MMTS and allow protein resuspension by dissolving precipitate in 300 µl of binding buffer (100 mM HEPES, 1.0 mM EDTA, 1% SDS, pH 7.5). After removal of 20 µl for input analysis, the remaining blocked proteins were divided into two tubes and treated with either 0.3 M hydroxylamine (NH_2OH; Scientific Laboratory Supplies) or 0.3 M NaCl, pH 7.5. Thiopropyl-Sepharose beads were rehydrated in a 1:1 slurry in binding buffer, and 50 µl of beads was added to each tube, incubating for 2.5 h at room temperature. After bead capture, the samples were centrifuged at 13,000 × *g* for 1 min and washed five times in binding buffer. The proteins were then eluted in 50 µl of 2× SDS-LB heated to 60 °C for 10 min. Proteins were analysed by 10% SDS-PAGE, loading 10 ul of input sample and 20 ul of eluted proteins and probed by Western blot for anti-FLAG. For quantitation, signals from the corresponding +NH_2OH lane were first normalised to the input signal for that assay. Data for the effect of the respective thioesterase was then expressed as a percentage of S-acylation of the corresponding ZERO or STREX-C53:54:56A channel expressed alone.

Membrane Potential Assay

Membrane potential assays were carried out as detailed previously for analysis of BK channel activity in HEK293 cells (23, 30). Transfected HEK293 cells were plated into a 96 well poly-d-lysine coated, black walled, clear bottom plate (Greiner) and assayed 48 h post-transfection. Cells were incubated with FLIPR® Membrane Potential Blue Dye (Molecular Devices, Sunnyvale, CA) containing 2 mM $CaCl_2$, for 30 min at room temperature. Assays were performed using the Flexstation R II system (Molecular Devices) at 22 °C by addition of the calcium ionophore ionomycin (0.83 µM final) after 16s. Fluorescent measurements as relative fluorescence units (RFU) were determined over a period of 180s. In this assay an increase in BK channel activity results in a hyperpolarisation which is detected as a decrease in fluorescence and is fully blocked by the specific 1 µM of the BK channel inhibitor paxilline (23). The assay is optimised to drive BK channel activation by elevation of intracellular free calcium that peaks approximately 40s following ionomycin addition before declining (23). As S-acylated STREX channels show increased apparent calcium sensitivity, without a significant change in voltage sensitivity compared to de-acylated STREX-C645:646A channels (17-19, 23), the peak calcium induced hyperpolarising response at ~ 50s represents the most sensitive component of the assay to discriminate functional S-acylation of STREX channels. To compare between conditions the RFU for each well was first normalised to its basal (pre ionomycin stimulus) RFU over the first 16s or recording as shown in Figure 5A. To allow quantification between experiments, as in Figure 5B, the peak hyperpolarising response in STREX expressing cells in each experiment was determined and subtracted from the corresponding HEK293 control and the peak response then expressed as a fraction of the peak hyperpolarisation in cells expressing STREX channels alone.

Statistics

The data are expressed as Mean ± SD, n = number of independent experiments. Statistical analysis was performed, as appropriate, by one ANOVA with Sidak post hoc multiple comparison tests for multiple comparisons of parametric data and using Kruskal Wallis test with Dunn's post-hoc test for non-parametric data (GraphPad Prism 8). Significant differences between groups were defined at * $p < 0.05$ and ** $p < 0.01$.

Data availability

All data are presented in the article, or are available from the corresponding author (Michael J Shipston, University of Edinburgh, mike.shipston@ed.ac.uk) on request.

Acknowledgements

We are grateful to Dr Anisha Kubasik-Thayil and the IMPACT imaging facility for assistance with confocal microscopy. Anna Boath assisted in the generation of the Δ19-ABHD17a construct. This work was generously supported by grants from The Wellcome Trust, British Heart Foundation and Medical Research Council to MJS.

Conflict of interest statement

The authors declare that they have no conflicts of interest with the contents of this article.

References

1. Chamberlain, L. H., and Shipston, M. J. (2015) The physiology of protein S-acylation. *Physiol. Rev.* **95**, 341–376
2. Shipston, M. J. (2011) Ion channel regulation by protein palmitoylation. *J. Biol. Chem.* **286**, 8709–8716
3. Lanyon-Hogg, T., Faronato, M., Serwa, R. A., and Tate, E. W. (2017) Dynamic Protein Acylation: New Substrates, Mechanisms, and Drug Targets. *Trends Biochem. Sci.* **42**, 566–581
4. Zaballa, M. E., and van der Goot, F. G. (2018) The molecular era of protein S-acylation: spotlight on structure, mechanisms, and dynamics. *Crit. Rev. Biochem. Mol. Biol.* **53**, 420–451
5. Rana, M. S., Kumar, P., Lee, C. J., Verardi, R., Rajashankar, K. R., and Banerjee, A. (2018) Fatty acyl recognition and transfer by an integral membrane S-acyltransferase. *Science 359: e*aao6326
6. Greaves, J., and Chamberlain, L. H. (2011) DHHC palmitoyl transferases: substrate interactions and (patho)physiology. *Trends Biochem. Sci.* **36**, 245–253
7. Linder, M. E., and Deschenes, R. J. (2007) Palmitoylation: policing protein stability and traffic. *Nat. Rev. Mol. Cell Biol.* **8**, 74–84
8. Won, S. J., Cheung, M., Kit, S., and Martin, B. R. (2018) Critical Reviews in Biochemistry and Molecular Biology Protein depalmitoylases Protein depalmitoylases. *Crit. Rev. Biochem. Mol. Biol.* 10.1080/10409238.2017.1409191
9. Duncan, J. A., and Gilman, A. G. (1998) A cytoplasmic acyl-protein thioesterase that removes palmitate from G protein alpha subunits and p21(RAS). *J. Biol. Chem.* **273**, 15830–15837
10. Tomatis, V. M., Trenchi, A., Gomez, G. A., and Daniotti, J. L. (2010) Acyl-Protein Thioesterase 2 Catalizes the Deacylation of Peripheral Membrane-Associated GAP-43. *PLoS One*. **5**, e15045
11. Lin, D. T. S., and Conibear, E. (2015) ABHD17 proteins are novel protein depalmitoylases that regulate N-Ras palmitate turnover and subcellular localization. *Elife*. **4**, e11306
12. Yokoi, N., Fukata, Y., Sekiya, A., Murakami, T., Kobayashi, K., and Fukata, M. (2016) Identification of PSD-95 Depalmitoylating Enzymes. *J. Neurosci.* **36**, 6431–6444
13. Tortosa, E., Adolfs, Y., Fukata, M., Pasterkamp, R. J., Kapitein, L. C., and Hoogenraad, C. C. (2017) Dynamic Palmitoylation Targets MAP6 to the Axon to Promote Microtubule Stabilization during Neuronal Polarization. *Neuron*. **94**:809-825
14. Remsberg, J. R., Suciu, R. M., Zambetti, N. A., Hanigan, T. W., Ari, J., Inguva, A., Long, A., Ngo, N., Lum, K. M., Henry, C. L., Richardson, S. K., Predovic, M., Huang, B., Howell, A. R., and Niphakis, M. J. (2020) ABHD17 enzymes regulate dynamic plasma membrane palmitoylation and N-Ras-dependent cancer growth bioRxiv 2020.05.21.108316
15. Tian, L., McClafferty, H., Knaus, H.-G. H.-G., Ruth, P., and Shipston, M. J. (2012) Distinct acyl protein transferases and thioesterases control surface expression of calcium-activated potassium channels. *J. Biol. Chem.* **287**, 14718–14725
16. Duncan, P. J., Bi, D., McClafferty, H., Chen, L., Tian, L., and Shipston, M. J. (2019) S -Acylation controls functional coupling of BK channel pore-forming α-subunits and β1-subunits. *J. Biol. Chem.* **294**, 12066–12076
17. Tian, L., Jeffries, O., McClafferty, H., Molyvdas, A., Rowe, I. C. M. I. C. M., Saleem, F., Chen, L., Greaves, J., Chamberlain, L. H., Knaus, H.-G., Ruth, P., and Shipston, M. J. (2008) Palmitoylation gates phosphorylation-dependent regulation of BK potassium channels. *Proc. Natl. Acad. Sci. U. S. A.* **105**, 21006–21011
18. Tian, L., McClafferty, H., Jeffries, O., and Shipston, M. J. (2010) Multiple palmitoyltransferases are required for palmitoylation-dependent regulation of large conductance calcium- and voltage-activated potassium channels. *J. Biol. Chem.* **285**, 23954–23962
19. Jeffries, O., Tian, L., McClafferty, H., and Shipston, M. J. (2012) An electrostatic switch controls palmitoylation of the large conductance voltage- and calcium-activated potassium (BK) channel. *J. Biol. Chem.* **287**, 1468–1477
20. Zhou, X., Wulfsen, I., Korth, M., McClafferty, H., Lukowski, R., Shipston, M. J., Ruth, P., Dobrev, D., and Wieland, T. (2012) Palmitoylation and membrane association of the stress axis regulated insert (STREX) controls BK channel regulation by protein kinase C. *J. Biol. Chem.* **287**, 32161–32171
21. Yokoi, N., Fukata, Y., Sekiya, A., Murakami, T., Kobayashi, K., and Fukata, M. (2016) Identification of PSD-95 Depalmitoylating Enzymes. *J. Neurosci.* **36**, 6431–6444
22. Dudem, S., Large, R. J., Kulkarni, S., McClafferty, H., Tikhonova, I. G., Sergeant, G. P., Thornbury, K. D., Shipston, M. J., Perrino, B. A., and Hollywood, M. A. (2020) LINGO1 is a regulatory subunit of large conductance, Ca2+-activated potassium channels. *Proc. Natl. Acad.*

Sci. U. S. A. **117**, 2194–2200
23. Saleem, F., Rowe, I. C. M., and Shipston, M. J. (2009) Characterization of BK channel splice variants using membrane potential dyes. *Br. J. Pharmacol.* **156**, 143–152
24. Chen, L., Jeffries, O., Rowe, I. C. M., Liang, Z., Knaus, H.-G., Ruth, P., and Shipston, M. J. (2010) Membrane trafficking of large conductance calcium-activated potassium channels is regulated by alternative splicing of a transplantable, acidic trafficking motif in the RCK1-RCK2 linker. *J. Biol. Chem.* **285**:33307-33314
25. Won, S. J., Davda, D., Labby, K. J., Hwang, S. Y., Pricer, R., Majmudar, J. D., Armacost, K. A., Rodriguez, L. A., Rodriguez, C. L., Chong, F. S., Torossian, K. A., Palakurthi, J., Hur, E. S., Meagher, J. L., Brooks, C. L., Stuckey, J. A., and Martin, B. R. (2016) Molecular Mechanism for Isoform-Selective Inhibition of Acyl Protein Thioesterases 1 and 2 (APT1 and APT2). *ACS Chem. Biol.* **11**, 3374–3382
26. Amara, N., Foe, I. T., Onguka, O., Garland, M., and Bogyo, M. (2019) Synthetic Fluorogenic Peptides Reveal Dynamic Substrate Specificity of Depalmitoylases. *Cell Chem. Biol.* **26**, 35-47.e7
27. Tortosa, E., Adolfs, Y., Fukata, M., Pasterkamp, R. J., Kapitein, L. C., and Hoogenraad, C. C. (2017) Dynamic Palmitoylation Targets MAP6 to the Axon to Promote Microtubule Stabilization during Neuronal Polarization. *Neuron*. **94**, 809-825.e7
28. Kathayat, R. S., Cao, Y., Elvira, P. D., Sandoz, P. A., Zaballa, M. E., Springer, M. Z., Drake, L. E., Macleod, K. F., Van Der Goot, F. G., and Dickinson, B. C. (2018) Active and dynamic mitochondrial S-depalmitoylation revealed by targeted fluorescent probes. *Nat. Commun.* **9**:334
29. Kim, S., Lee, B.-C., Lee, A.-R., Won, S., and Park, C.-S. (2014) Effects of palmitoylation on the diffusional movement of BKCa channels in live cells. *FEBS Lett.* **588**, 713–719
30. Jeffries, O., Geiger, N., Rowe, I. C. M., Tian, L., McClafferty, H., Chen, L., Bi, D., Knaus, H.-G., Ruth, P., and Shipston, M. J. (2010) Palmitoylation of the S0-S1 linker regulates cell surface expression of voltage- and calcium-activated potassium (BK) channels. *J. Biol. Chem.* **285**, 33307–33314
31. Forrester, M. T., Hess, D. T., Thompson, J. W., Hultman, R., Moseley, M. A., Stamler, J. S., and Casey, P. J. (2011) Site-specific analysis of protein S-acylation by resin-assisted capture. *J. Lipid Res.* **52**, 393–398

Figure legends

Figure 1
ABHD17a controls plasma membrane association of BK channel STREX domain

A) Schematic of pore-forming subunit of the STREX BK channel splice variant indicating the two S-acylated domains of the channel: the S0-S1 loop present in all channel variants, and the alternatively spliced STREX insert in the intracellular C-terminus of the channel located between the two regulator of potassium conductance (RCK) domains. **B**) The isolated S-acylated STREX-CRD fusion protein is associated with the plasma membrane when expressed in HEK293 cells and remains cytosolic when deacylated. **C**) Representative confocal sections of HEK293 cells expressing the STREX-CRD (as a -GFP fusion protein) and upon co-expression with ABHD17a. Scale bars are 2 μm. **D**) Immunostaining of populations of HEK293 cells in 96 wells for overexpressed Flag-tagged putative acyl thioesterases from the ABHD and Lypla families. **E**) Quantification of membrane expression of STREX-CRD, as a -GFP fusion protein, in HEK293 upon co-expression with ABHD and Lypla acyl thioesterase family members. Data are expressed as the fraction of cells expressing STREX-CRD at the plasma membrane in comparison to cells expressing STREX-CRD alone. Data are Means ± SD, n = 23-54 independent experiments per group. ** $p < 0.01$, * $p < 0.05$ compared to STREX-CRD alone, non-parametric Kruskal Wallis with post hoc Dunn's test.

Figure 2
ABHD17a deacylates the BK channel STREX, but not S0-S1 loop, domain

Representative Western blots from an acyl-RAC assay of **A**) ZERO BK channel variant that lacks the STREX domain or **B**) the STREX-C53:54:56A mutant that cannot be S-acylated in the S0-S1 loop, expressed in HEK293 cells alone or with ABHD17a or ABHD17c. Cell lysate input to the acyl-RAC assay is shown together with pull downs following cleavage of thioester bond with hydroxylamine ($+NH_2OH$) or in salt control ($-NH_2OH$). Quantification of S-acylation of **C**) ZERO or **D**) STREX-C53:54:56A in the presence of ABHD17a or ABHD17c. Data are expressed as percentage of S-acylation of corresponding ZERO or STREX-C53:54:56A channel alone (Control) as Means ± SD, n = 4 independent experiments per group. ** $p < 0.01$, * $p < 0.05$ compared to STREX-C53:54:56A alone, non-parametric Kruskal Wallis with post hoc Dunn's test.

Figure 3
ABHD17a dependent deacylation does not control BK channel surface expression

A) Representative on-cell western assay of cell surface expression of epitope tagged BK ZERO, ZERO-C53:54:56A and STREX channels alone or co-expressed with wild-type β1 or co-expressed with wild-type ABHD17a, the catalytically inactive ABHD17a mutant (ABHD17a-mut) or the N-terminally truncated, targeting deficient ABHD17a (Δ19-ABHD17a). Surface BK channel was quantified using an extracellular FLAG-tag (green) while total BK expression was measured using an intracellular -HA tag (red) following cell permeabilization. Four replicates from an individual experiment are shown. (**B to E**) Quantification of corresponding BK channel surface expression in the presence of acyl thioesterases and their related mutants as in A) and expressed as a fraction of the corresponding BK channel subunit expressed alone. Data are Means ± SD, n = 5-17 independent experiments per group. ** $p < 0.01$, * $p < 0.05$ compared to corresponding BK channel group alone, non-parametric Kruskal Wallis with post hoc Dunn's test.

Figure 4
ABHD17a does not control BK channel internalisation

A) Schematic of internalisation assay and B) representative images from an internalisation assay of epitope tagged ZERO BK channels alone or co-expressed with ABHD17a and it mutants in HEK293 cells. Internalised BK α-subunit was quantified, after 60 min at 37°C, using the extracellular FLAG- tag (green) following acid-strip of surface staining in non-permeabilised cells and normalised to surface expression at time zero. Four replicates from an individual experiment are shown. (**C**) Quantification of BK channel α-subunit internalisation as a percentage of initial total surface expression. Data are Means ± SD (n = 4 independent experiments per group).

Figure 5
ABHD17a mediated deacylation of the STREX domain inhibits STREX channel function

A) Representative experimental time courses of ionomycin (1μM started at 16s, horizontal grey bar) induced changes in membrane potential of HEK293 cells transfected with STREX channel variants and

ABHD17a using a 96-well format cell population Flexstation membrane potential assy. Positive changes in relative fluorescence units (RFU) denote membrane depolarisation, whereas negative changes in RFU reflect membrane hyperpolarisation. Assays were performed in physiological ion gradients with 2mM extracellular calcium. Data are Means ± SD from a single typical independent experiment with 8 experimental replicates. **B**) Quantification of peak hyperpolarisation response to ionomycin in membrane potential assays expressed as a fraction of the peak hyperpolarisation in cells expressing STREX channels alone. Data are Means ± SD, n = 5-20 per group. ** $p < 0.01$ compared to STREX, non-parametric Kruskal Wallis with post hoc Dunn's test.

Figure 6
Distinct acyl protein thioesterases control deacylation at distinct sites in BK channels
A) Schematic of the STREX variant of the BK channel pore forming subunit (Kcnma1) and sites of S-acylation. The STREX domain is deacylated by Abhd17a and the S0-S1 domain by Lypla1. B) Amino acid sequence of other targets for ABHD17 acyl thioesterases showing the 10 most vicinal residues surrounding S-acylated cysteines. Mouse sequences and numbering is used throughout and include proteins with S-acylation at the i) N-terminus including Psd-95 (11, 12), Gap-43 (12) and Map6 (27); ii) internal/intracellular loop cysteines such as Mpp6 (14) and the STREX variant of Kcnma1 shown here and; iii) cysteines towards the C-terminus of proteins including H-Ras and N-Ras (11, 12).

Fig 1

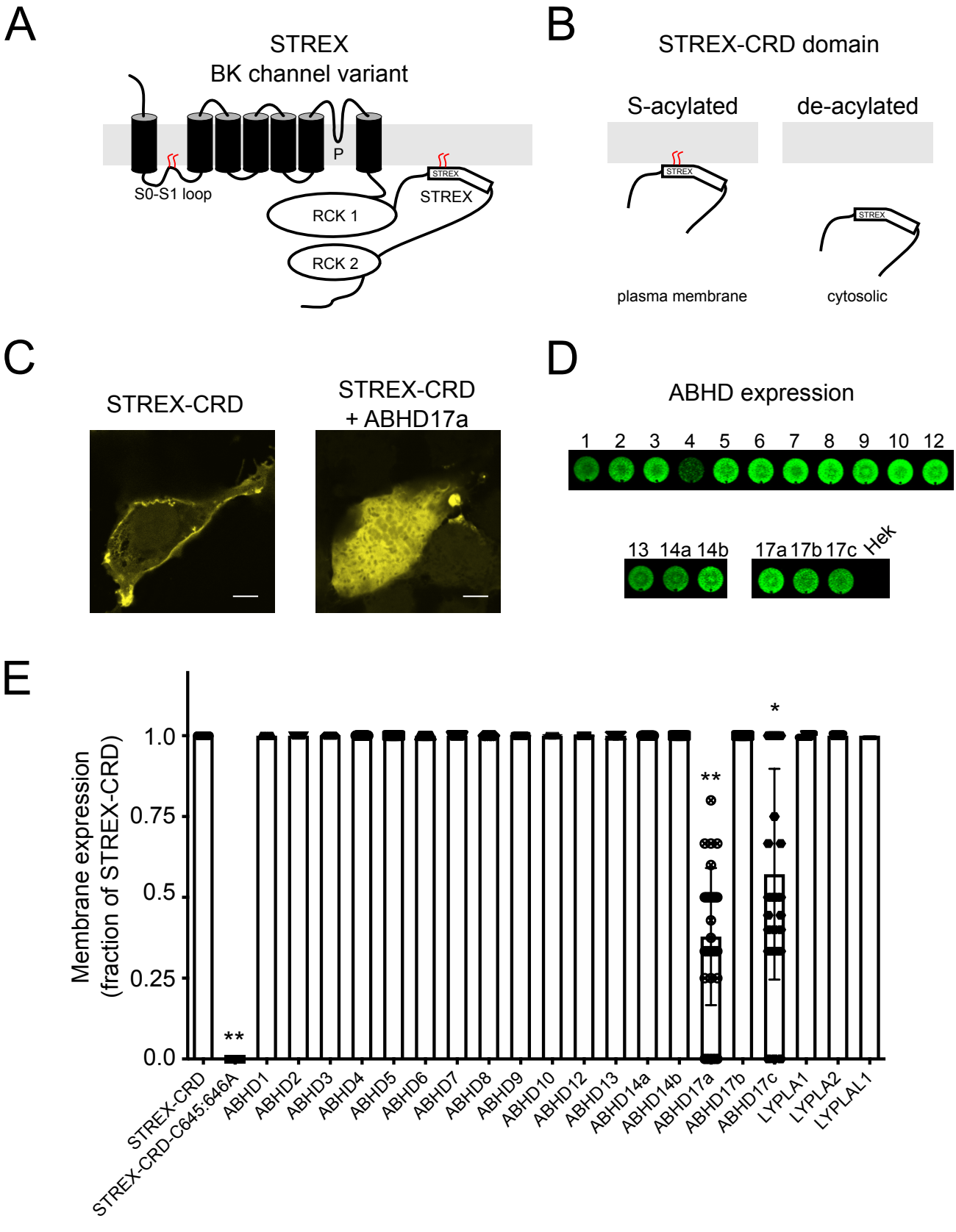
A
STREX
BK channel variant
S0-S1 loop
P
RCK 1
RCK 2
STREX
B
STREX-CRD domain
S-acylated
de-acylated
plasma membrane
cytosolic
C
STREX-CRD
STREX-CRD
+ ABHD17a
D
ABHD expression
1 2 3 4 5 6 7 8 9 10 12
13 14a 14b
17a 17b 17c Hek
E
Membrane expression
(fraction of STREX-CRD)
1.0
0.75
0.5
0.25
0.0
**
**
*
STREX-CRD
STREX-CRD-C645:646A
ABHD1
ABHD2
ABHD3
ABHD4
ABHD5
ABHD6
ABHD7
ABHD8
ABHD9
ABHD10
ABHD12
ABHD13
ABHD14a
ABHD14b
ABHD17a
ABHD17b
ABHD17c
LYPLA1
LYPLA2
LYPLAL1

Fig 2

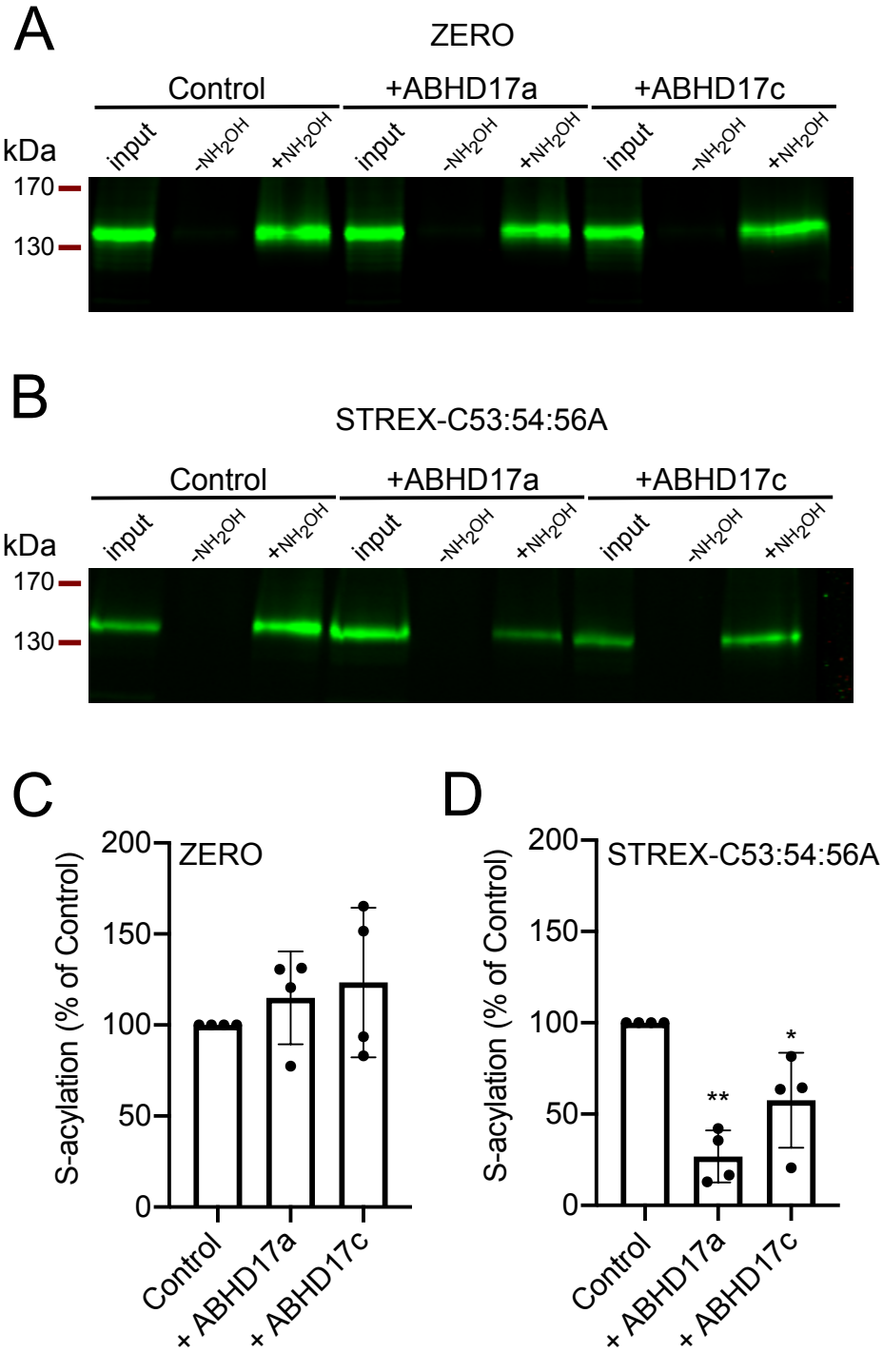
A
ZERO
Control
+ABHD17a
+ABHD17c
kDa
input
-NH2OH
+NH2OH
170
130
B
STREX-C53:54:56A
C
ZERO
S-acylation (% of Control)
200
150
100
50
0
Control
+ ABHD17a
+ ABHD17c
D
STREX-C53:54:56A
**
*

Fig 3

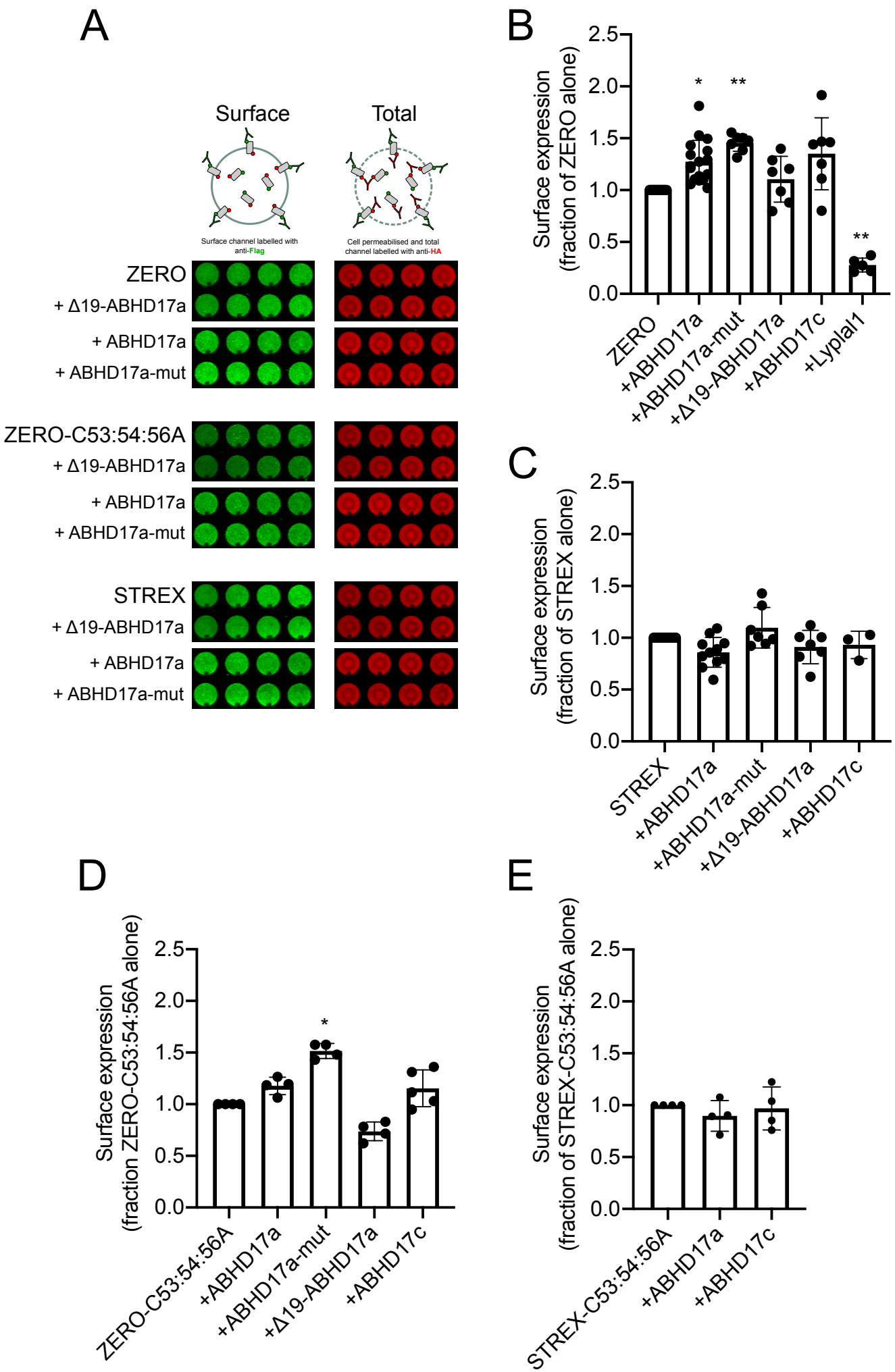
A
Surface
Total
Surface channel labelled with anti-Flag
Cell permeabilised and total channel labelled with anti-HA
ZERO
+ Δ19-ABHD17a
+ ABHD17a
+ ABHD17a-mut
ZERO-C53:54:56A
+ Δ19-ABHD17a
+ ABHD17a
+ ABHD17a-mut
STREX
+ Δ19-ABHD17a
+ ABHD17a
+ ABHD17a-mut
B
Surface expression (fraction of ZERO alone)
2.5
2.0
1.5
1.0
0.5
0.0
*
**
**
ZERO
+ABHD17a
+ABHD17a-mut
+Δ19-ABHD17a
+ABHD17c
+Lyplal1
C
Surface expression (fraction of STREX alone)
2.5
2.0
1.5
1.0
0.5
0.0
STREX
+ABHD17a
+ABHD17a-mut
+Δ19-ABHD17a
+ABHD17c
D
Surface expression (fraction ZERO-C53:54:56A alone)
2.5
2.0
1.5
1.0
0.5
0.0
*
ZERO-C53:54:56A
+ABHD17a
+ABHD17a-mut
+Δ19-ABHD17a
+ABHD17c
E
Surface expression (fraction of STREX-C53:54:56A alone)
2.5
2.0
1.5
1.0
0.5
0.0
STREX-C53:54:56A
+ABHD17a
+ABHD17c

Fig 4

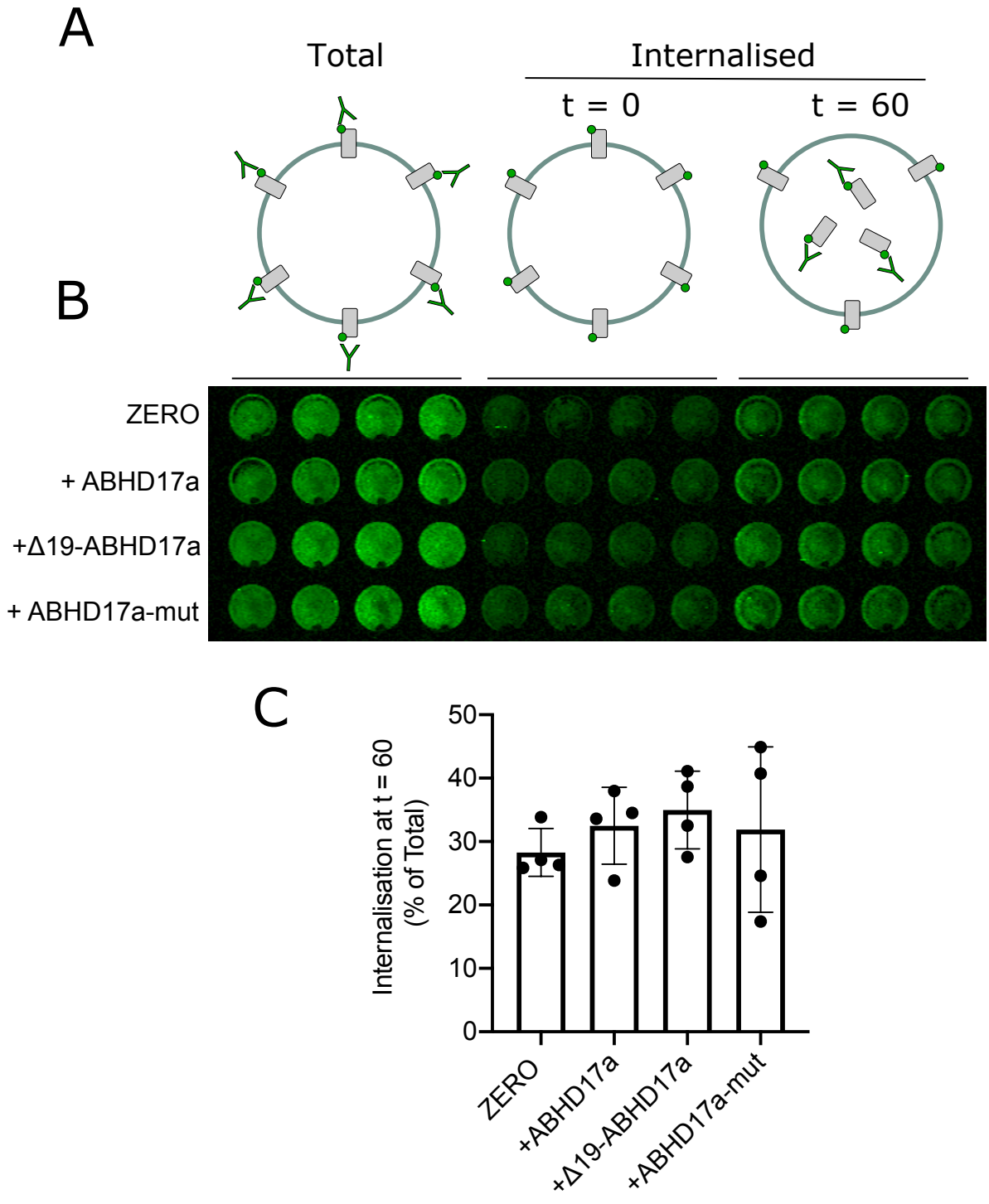
A
Total
Internalised
t = 0
t = 60
B
ZERO
+ ABHD17a
+Δ19-ABHD17a
+ ABHD17a-mut
C
Internalisation at t = 60
(% of Total)
50
40
30
20
10
0
ZERO
+ABHD17a
+Δ19-ABHD17a
+ABHD17a-mut

Fig 5

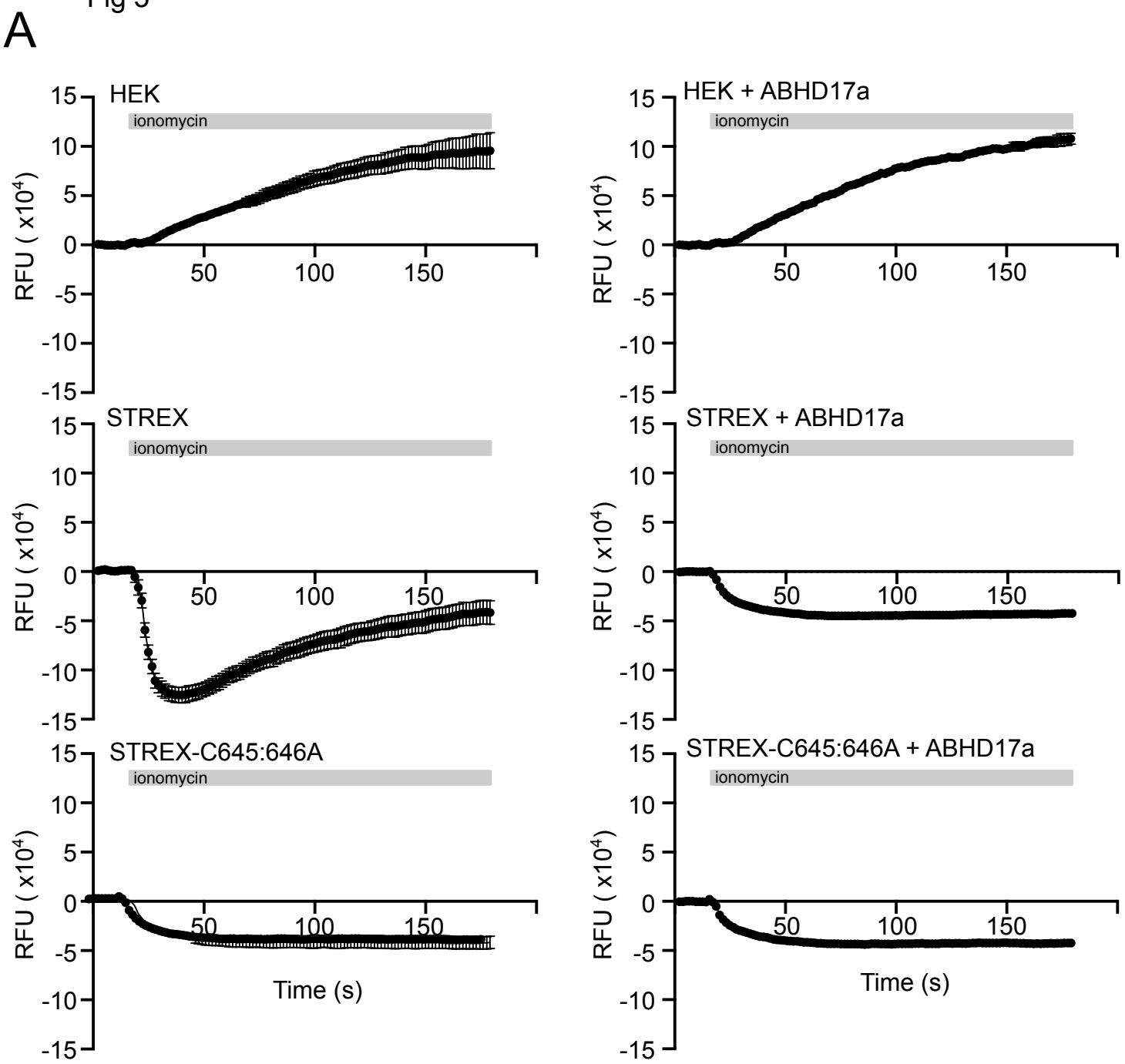
A
HEK
ionomycin
HEK + ABHD17a
ionomycin
STREX
ionomycin
STREX + ABHD17a
ionomycin
STREX-C645:646A
ionomycin
STREX-C645:646A + ABHD17a
ionomycin
RFU (x10^4)
Time (s)

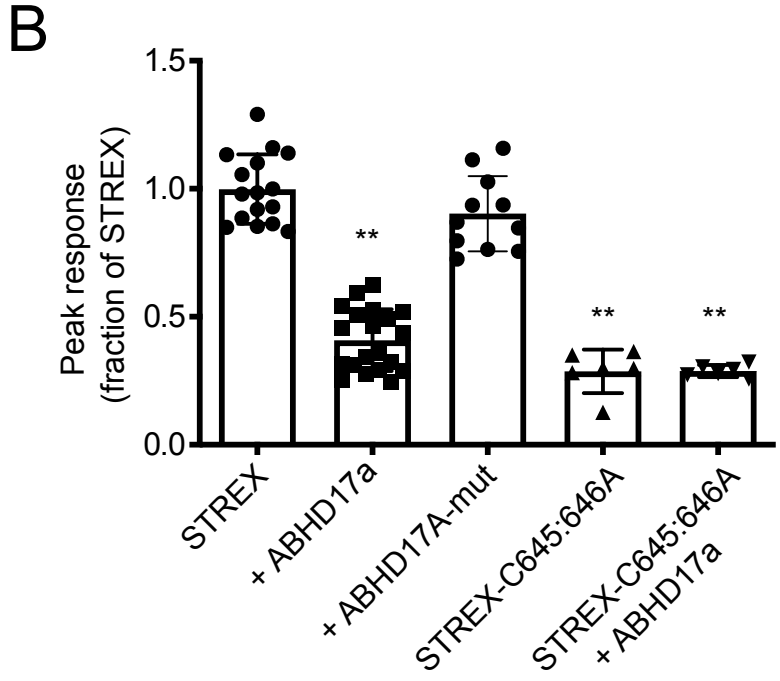
B
Peak response
(fraction of STREX)
1.5
1.0
0.5
0.0
**
**
**
STREX
+ ABHD17a
+ ABHD17A-mut
STREX-C645:646A
STREX-C645:646A
+ ABHD17a

Fig 6

A

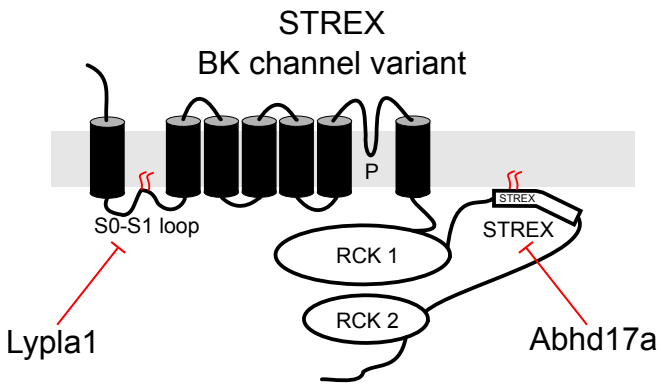

B

N-terminal

Psd-95	MDC^{3}LC^{5}IVTTKKYRYQ...
Map6	MAWPC^{5}ITRAC^{10}C^{11}IARFWNQLDK...
Gap-43	MLC^{3}C^{4}MRRTKQVEKN...

Internal/intracellular loop

Mpp6	...RRDWDNSGPFC^{311}GTISNKKKKK...
Kcnma1 (STREX)	...MSIYKRMRRAC^{645}C^{646}FDCGRSERDC...

C-terminal

N-Ras	...LNSSDDGTQGC^{181}MGSPCVVM
H-Ras	...LNPPDESGPGC^{181}MSC^{184}KCVLS